Histamine Suppresses Fibulin-5 and Insulin-like Growth Factor-II Receptor Expression in Melanoma

Zoltan Pos,[1] Zoltan Wiener,[1] Peter Pocza,[1] Melinda Racz,[1] Sara Toth,[1] Zsuzsanna Darvas,[1] Viktor Molnar,[1] Hargita Hegyesi,[1] and Andras Falus[1,2]

[1]Department of Genetics, Cell, and Immunobiology, and [2]Immunogenomics Research Group, Hungarian Academy of Sciences, Semmelweis University, Budapest, Hungary

Abstract

We previously showed that transgenic enhancement of histamine production in B16-F10 melanomas strongly supports tumor growth in C57BL/6 mice. In the present study, gene expression profiles of transgenic mouse melanomas, secreting different amounts of histamine, were compared by whole genome microarrays. Array results were validated by real-time PCR, and genes showing histamine-affected behavior were further analyzed by immunohistochemistry. Regulation of histamine-coupled genes was investigated by checking the presence and functional integrity of all four known histamine receptors in experimental melanomas and by administering histamine H1 receptor (H1R) and H2 receptor (H2R) antagonists to tumor-bearing mice. Finally, an attempt was made to integrate histamine-affected genes in known gene regulatory circuits by *in silico* pathway analysis. Our results show that histamine enhances melanoma growth via H1R rather than through H2R. We show that H1R activation suppresses RNA-level expression of the tumor suppressor insulin-like growth factor II receptor (IGF-IIR) and the antiangiogenic matrix protein fibulin-5 (FBLN5), decreases their intracellular protein levels, and also reduces their availability in the plasma membrane and extracellular matrix, respectively. Pathway analysis suggests that because plasma membrane-bound IGF-IIR is required to activate matrix-bound, latent transforming growth factor-β1, a factor suggested to sustain FBLN5 expression, the data can be integrated in a known antineoplastic regulatory pathway that is suppressed by H1R. On the other hand, we show that engagement of H2R also reduces intracellular protein pools of IGF-IIR and FBLN5, but being a downstream acting posttranslational effect with minimal consequences on exported IGF-IIR and FBLN5 protein levels, H2R is rather irrelevant compared with H1R in melanoma. [Cancer Res 2008;68(6):1997–2005]

Introduction

Cancer progression is a highly complicated process, the exact mechanism of which is still not completely understood. Recently published data obtained from different clinical and experimental studies strongly support the old proposition originally suggested by Virchow in the 19th century that chronic local inflammation might represent a key event in the early steps of tumorigenesis (1). Chronic inflammations, typically sustained by unresolved infections or permanent tissue stress, are apparently capable of inducing mutagenesis by local overproduction of reactive oxygen and nitrogen intermediates (2) and bypassing p53-mediated cell cycle control mechanisms via inflammatory cytokines such as macrophage migration inhibitory factor (3). In addition, chronic inflammation enhances invasive potential of tumor cells by inducing matrix reorganization affecting collagen synthesis (4) and enhancing matrix breakdown by matrix metalloproteinases (MMP) like MMP-3 or MMP-9 (5). Therefore, cancer cells often highjack the molecular machinery of inflammation [e.g., when they facilitate neoplastic motility by overexpressing some chemokine receptors (6), or as they foster angiogenesis by secreting several inflammatory chemokines of the CXCL family (7)]. Finally, chronic inflammation is deeply involved in the induction of neoplastic immunosuppression, as well (8).

Histamine is a common mediator of inflammatory reactions, but it has potent immunomodulatory effects, too (9). It is typically secreted by mast cells and basophils and, to a lesser extent, by many different, even nonimmune, cell types (9). Intensive production and subsequent secretion of this inflammatory mediator have been reported in many rapidly dividing tissues and neoplasms (10–12), including melanoma (13). These observations provided a rationale for many research projects investigating the neoplastic and immunomodulatory effects of histamine during tumorigenesis (14, 15) and the use of histamine receptor antagonists in tumor therapy. We previously showed that transgenic modification of neoplastic histamine production heavily influences tumor progression of mouse experimental melanomas *in vivo* (16). By modifying the levels of L-histidine decarboxylase (HDC), the sole enzyme responsible for histamine production, we introduced novel variants of the B16-F10 mouse melanoma cell line, displaying diminished (B16-F10 HDC-A), unmodified (B16-F10 HDC-M), or enhanced (B16-F10 HDC-S) capacities to produce and secrete histamine. Using this model, we showed that histamine secretion by tumor cells markedly enhances experimental tumor growth of B16-F10 cells in C57BL/6 mice. In this study, novel melanoma genes affected by histamine, which are potentially responsible for histamine-dependent acceleration of tumor growth, were identified by global gene expression profiling.

Materials and Methods

Animals. Eight- to 12-week-old, specific pathogen-free female C57BL/6 mice were obtained from the Hungarian National Institute of Oncology and maintained under sterile conditions in our animal care facility. Animals were kept with free access to food and water.

Note: Supplementary data for this article are available at Cancer Research Online (http://cancerres.aacrjournals.org/).

Part of a series: This article is based on our previous publication in Cancer Research [Cancer Res. 2005 May 15;65(10):4458-66, Pos et al.] and hence it can be regarded as part of a series.

Requests for reprints: Andras Falus, Immunogenomics Research Group, Hungarian Academy of Sciences, Semmelweis University, 4 Nagyvarad ter, H-1089 Budapest, Hungary. Phone: 36-1-210-2929; E-mail: faland@dgci.sote.hu.

doi:10.1158/0008-5472.CAN-07-2816

Cells. Nine novel B16-F10 subclones, engineered to produce and secrete different amounts of histamine, constitutively expressing an antisense mouse HDC mRNA (B16-F10 HDC-A1, -A2, and -A3), a mock RNA sequence (B16-F10 HDC-M1, -M2, and -M3), or the full-length sense mouse HDC ORF (B16-F10 HDC-S1, -S2, and -S3), were generated as described elsewhere (16). In this study, based on data published about their individual histamine secretion levels (16), the subclones -A1, -M2, and -S2 were chosen for further evaluation and will be referred to as B16-F10 HDC-A, B16-F10 HDC-M, and B16-F10 HDC-S for clarity. Cells were cultured in high-glucose DMEM in the presence of 2% glutamine, 10% FCS (Invitrogen-Gibco), 160 μg/mL gentamicin, and 400 μg/mL hygromycin B (Merck-Calbiochem) in a humidified 5% CO_2 atmosphere at 37°C.

***In vitro* histamine receptor agonist and antagonist assays.** For agonist assays, B16-F10 HDC-M cells were plated on 24-well plates at a density of 2×10^5 per well for H1 receptor (H1R) assays, or on six-well plates at a density of 5×10^5 per well for H2 receptor (H2R) assays, in duplicates. After 48 hours, cells were stimulated by the specific H1 and H2R agonists 2-pyridylethylamine dihydrochloride (Tocris) and amthamine dihydrobromide (Sigma-Aldrich), respectively. Both agonists were administered in concentrations of 10^{-3}, $10^{-4,}$ 10^{-5}, 10^{-6}, and 10^{-7} mol/L, and applied for 1 hour at 37°C, 5% CO_2. Then, cells were harvested and levels of intracellular inositol-monophosphate or cyclic AMP (cAMP) were determined with an IP-One ELISA (Cis-Bio) or a Parameter Cyclic AMP Assay (R&D), respectively, following the manufacturer's instructions.

In experiments with histamine receptor antagonists, 1×10^5 B16-F10 HDC-S cells were cultivated in the absence or presence of 10^{-6} mol/L loratadine or 10^{-6} mol/L famotidine (both from Sigma-Aldrich), in daily changed medium, for 1 week. FCS was omitted on the last 2 days of culture to remove exogenously added serum proteins from the supernatant. On day 7, supernatants were collected; the >30-kDa molecular weight soluble protein fraction was concentrated by an Amicon Ultracel-30 Membrane (Millipore-Chemicon); and the amount of secreted fibulin-5 (FBLN5) was determined by Western blotting in two independent experiments. Cells were nonenzimatically isolated at the end of the treatment period with PBS-buffered 0.02% EDTA, and used to determine surface insulin-like growth factor II (IGF-II) receptor (IGF-IIR) levels by flow cytometry in three independent experiments.

Graft tumor experiments. Stably transfected B16-F10 cells (2×10^5) were collected in a volume of 50-μL PBS per animal and injected s.c. in the shaved backs of C57BL/6 mice in groups of 10. At 6, 8, 10, 13, and 15 days after graft implantation, the longest and shortest radii (a and b, respectively) of tumors were determined with a microcaliper, and tumor size was calculated, assuming ellipsoidal tumor growth, using the formula $4/3ab^2\pi$. In experiments with histamine receptor antagonists, animals were additionally treated with a daily dose of loratadine (0.1, 1, or 10 mg/kg body weight/d) or famotidine (10, 100, or 1,000 mg/kg body weight/d) p.o., via drinking water. Statistical comparison of tumor growth rates was done by two-way ANOVA and Holm-Sidak test as post hoc test. At 15 days after grafting, all mice were sacrificed, and tumors were excised. Immediately after excision, tumor samples were stored at −80°C for RNA and protein isolation, or fixed in sterile 1× PBS containing 4% formaldehyde for histologic analysis.

RNA isolation and quality control. Total RNA isolation was carried out from six randomly chosen tumors per experimental group, using RNeasy columns (Qiagen). RNA yield and purity were determined with an ND1000 spectrophotometer (Nanodrop). RNA integrity was checked by capillary electrophoresis with an RNA Series II 6000 Nano Kit (Agilent Technologies) and a 2100 Bioanalyzer (Agilent). For microarray studies, equal amounts of randomly chosen RNA sample pairs were pooled. For real-time PCR studies, all tumor RNA samples were processed individually.

Microarray experiments. Array experiments were done in a two-color experimental design by comparing individual tumor samples via a uniform reference sample. One microgram of tumor-derived, pooled total RNA was mixed with an RNA Spike-In Kit (Agilent), reverse transcribed by a Low RNA Input Linear Amplification Kit (Agilent), and used for cyanine 5-CTP–labeled (Perkin-Elmer) cRNA synthesis in a linear amplification reaction. Successful labeling, cRNA yield, and purity were controlled on an ND1000 (Nanodrop) spectrophotometer. Next, 750 ng of cyanine 5-CTP–labeled cRNA per tumor sample were mixed with an equal amount of cyanine 3-CTP–labeled (Perkin-Elmer) uniform reference cRNA, generated from *in vitro* cultivated B16-F10 HDC-M cells as above, and hybridized to 44K Whole Mouse Genome Oligo Microarrays (Agilent). Array scanning, feature extraction, and data normalization were done with Agilent DNA Microarray Scanner and Feature Extraction Software 8.5 (Agilent). Data were then transferred for statistical evaluation in the GeneSpring software package (Agilent) with default normalization scenario for Agilent two-color arrays. Identification of gene sets differentially expressed between HDC-A–, HDC-M–, and HDC-S–transfected tumor groups was carried out by one-way ANOVA with Benjamini-Hochberg multiple testing correction. Tukey's all pairwise multiple comparison was applied as post hoc test. Microarray data have been deposited in National Center for Biotechnology Information Gene Expression Omnibus (GEO)[3] and are accessible through GEO Series accession no. GSE8541.

Real-time PCR. One microgram of total RNA per tumor sample was reverse transcribed using Random 6-mer Primers (Promega) and the Reverse Transcription System (Promega). cDNA aliquots were amplified by predeveloped TaqMan probe sets specific for mouse asparagine synthetase (ASNS), FBLN5, carbonic anhydrase 13 (CAR13), retroviral integration site 2 (RIS2), IGF-IIR, and hypoxanthine guanine phosphoribosyl transferase (HGPRT) as housekeeping internal standard. All probe sets were purchased from Applied Biosystems. Real-time primer extension was done on an ABI Prism 7000 thermal cycler (Applied Biosystems). HGPRT-normalized signal levels were calculated using the comparative C_t ($\Delta\ddot{A}C_T$) method and expressed in percents of the respective marker level measured in mock-transfected tumors. Statistical result evaluation was done by one-way ANOVAs supported by Holm-Sidak post hoc tests.

Western blotting. For protein isolation from experimental tumors, four randomly chosen tumors per experimental group were homogenized in a buffer containing 10 mmol/L Tris-HCl (pH 8.0), 10 mg/mL leupeptin, 0.5 mmol/L EGTA, 2% NaF, 1% Triton X-100, 25 mmol/L phenyl-methyl-sulfonyl-fluoride, and 2% Na-orthovanadate. Debris was removed by centrifugation, and protein yield was assessed by spectrophotometry. For protein isolation from cell culture supernatants, 200 μL of supernatant protein concentrate were dissolved in 800-μL buffer and processed as above. Then, 10-μg aliquots of heat-denatured, β-mercaptoethanol–treated protein samples were loaded on precast Ready Gels (Bio-Rad). Gels were blotted onto polyvinylidene difluoride membranes (Bio-Rad), blocked, and blots were probed with rabbit anti-mouse histamine H1R (1:200; Santa Cruz), rabbit anti-mouse histamine H2R or H3R (both 1:1,000; Alpha Diagnostic), goat anti-mouse histamine H4R (1:200; Santa Cruz), goat anti-human IGF-IIR (0.5 μg/mL; R&D), rabbit anti-human RIS2 (1:2,000; Bethyl), goat anti-mouse FBLN5 (1:2,000; Santa Cruz), or rat anti-mouse α-tubulin (1:4,000; AbD Serotec) antibodies, as stated. Blots were washed and secondary rabbit anti-goat IgG-horseradish peroxidase (HRP; 1:16,000), goat anti-rabbit IgG-HRP (1:10,000), or rabbit-anti rat IgG κ and λ chain HRP antibodies (1:10,000, all from Sigma-Aldrich) were applied, as appropriate. After subsequent washes, immunoreactive bands were visualized with the ECL-Plus Western blotting Detection System (GE Healthcare-Amersham). Image analysis was done using a Fluorchem 8000 image analysis platform (Alpha Innotech) and the ChemiImager 5500 image analysis software package (Alpha Innotech). Specific band size was determined with the Full Range Rainbow Molecular Weight Marker (GE Healthcare-Amersham).

Immunohistochemistry. Formalin-fixed and paraffin-embedded tissues of six randomly chosen tumors per experimental group were cut, mounted onto slides, and stained with standard H&E for gross histologic evaluation. For immunohistochemistry, deparaffinized specimens were blocked with nonimmune goat serum (DAKO) and incubated with rabbit anti-mouse ASNS (1:50; Epitomics), goat anti-human IGF-IIR (15 μg/mL; R&D), or goat anti-mouse FBLN5 primary antibodies (1:50; Santa Cruz). Washed specimens were incubated with goat anti-rabbit IgG-FITC or rabbit anti-goat

[3] http://www.ncbi.nlm.nih.gov/geo/

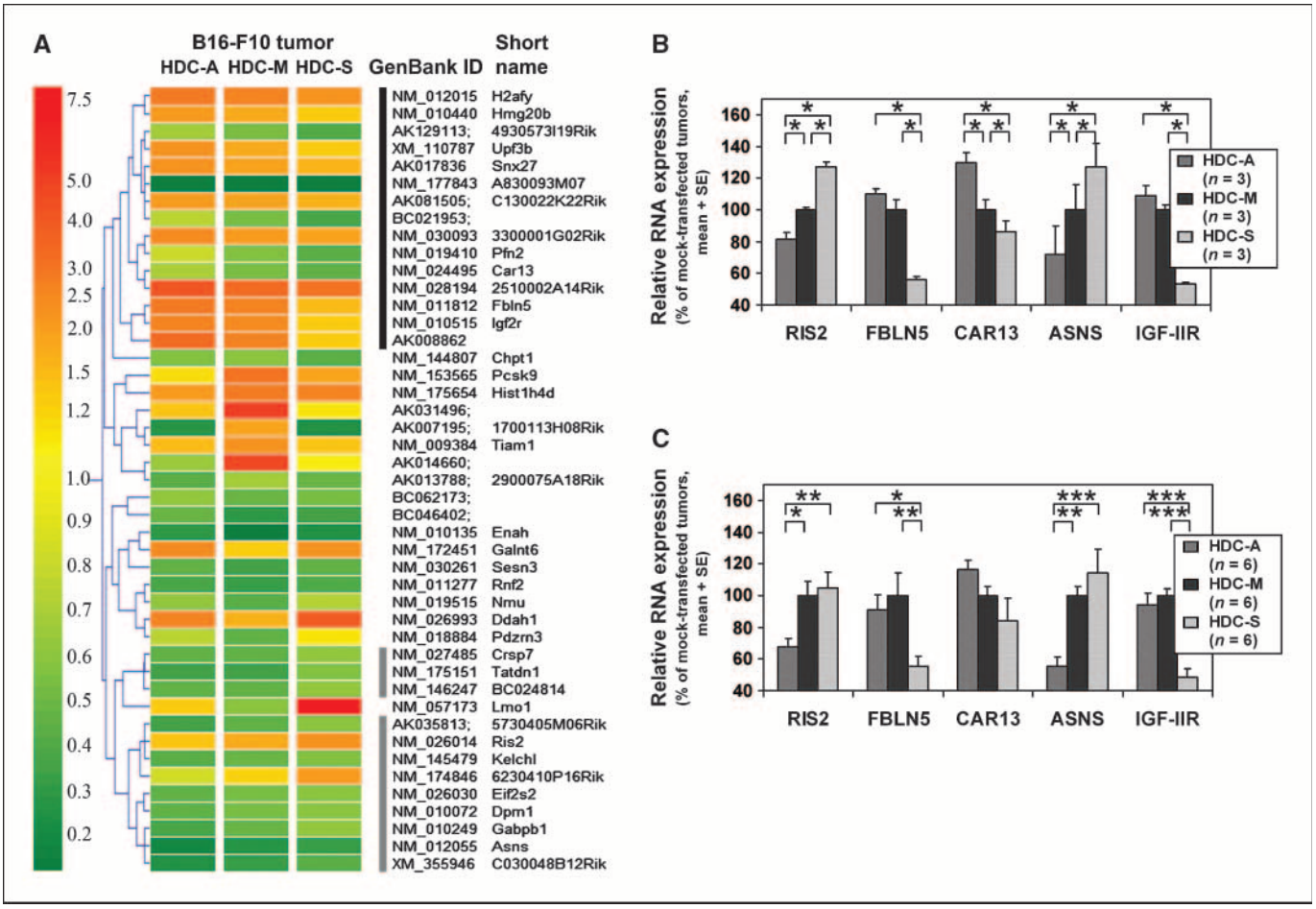

Figure 1. Global gene expression profiling of transgenic B16-F10 melanoma tumors with diminished, unmodified, and enhanced histamine production. *A,* color-coded gene expression data, GenBank IDs, and abbreviated names of 45 hierarchically clustered genes, all significantly affected by histamine in experimental B16-F10 mouse melanomas. Data are derived from three different tumor groups with suppressed (HDC-A), unmodified (HDC-M), and enhanced (HDC-S) histamine production, compared by 44K whole genome gene expression microarrays. *Black* and *gray bars,* gene clusters showing gradually down-regulated and up-regulated expression by histamine, respectively. For detailed information about displayed genes, see Supplementary data 3. *B,* detailed gene expression patterns, as determined by microarray analysis, of five histamine-affected genes involved in tumor progression. *C,* real-time PCR–based validation of the above microarray data. *, $P < 0.05$; **, $P < 0.01$; ***, $P < 0.001$, between individual groups as determined by a Tukey (*A*) or a Holm-Sidak test (*B*).

IgG-FITC secondary antibodies, as needed (both 1:150; Sigma-Aldrich), and washed again. Finally, cell nuclei were counterstained with daunorubicin (1:120; Sigma-Aldrich). Slides were mounted with coverslips and analyzed with an MRC 1024 confocal laser scanning microscope (Bio-Rad) at minimal ×10 magnification. Signal intensities were normalized using the LaserSharp2000 image acquisition software (Bio-Rad) by subtracting background fluorescence given by secondary antibodies only. No further image manipulation was done. Signal specificity was checked with blocking peptides, if available (for IGF-IIR and FBLN5). Signal intensities were determined densitometrically with the NIH Image software (Scion) by measuring three randomly chosen tumor areas per slide by minimal magnification (×40). Signal intensities were expressed in percents of the respective marker level measured in mock-transfected tumors. Statistics were done by applying one-way ANOVA and the Holm-Sidak post hoc test. Representative ×400 magnification sections of original micrographs were used for illustrative purposes.

Flow cytometry. Cells (10^6 per sample) were fixed in a PBS solution containing 4% paraformaldehyde, washed with PBS containing 1% bovine serum albumin (BSA) twice, and stained with 0.5-μg goat anti-human IGF-IIR antibody (R&D) for 45 minutes at +4°C. After two subsequent washes, cells were stained with FITC-conjugated rabbit anti-goat IgG antibody (Sigma-Aldrich) for 45 minutes at +4°C in the dark. After two additional washes, cells were resuspended in PBS-BSA and analyzed on a FACSCalibur flow cytometer (BD Biosciences). Results were evaluated with the Cell Quest Pro software (BD Biosciences). Specific signals were identified by comparing all measured signals with nonspecific background staining given by the secondary antibody only.

Pathway analysis. Identification and analysis of histamine-affected, functionally clustered gene networks was done with the Ingenuity Pathways Analysis system (Ingenuity Systems).[4]

General remarks. Unless otherwise stated, all materials were purchased from Sigma-Aldrich. For statistical analyses, $P < 0.05$ was considered statistically significant.

Results

Microarrays define histamine-affected gene clusters in mouse melanoma. Mouse 44K whole genome oligonucleotide expression arrays were used to identify gene expression signatures dose-dependently up-regulated or down-regulated by histamine in transgenic B16-F10 experimental melanoma tumors. In these experiments, stably transfected B16-F10 HDC-A, B16-F10 HDC-M,

[4] http://www.ingenuity.com

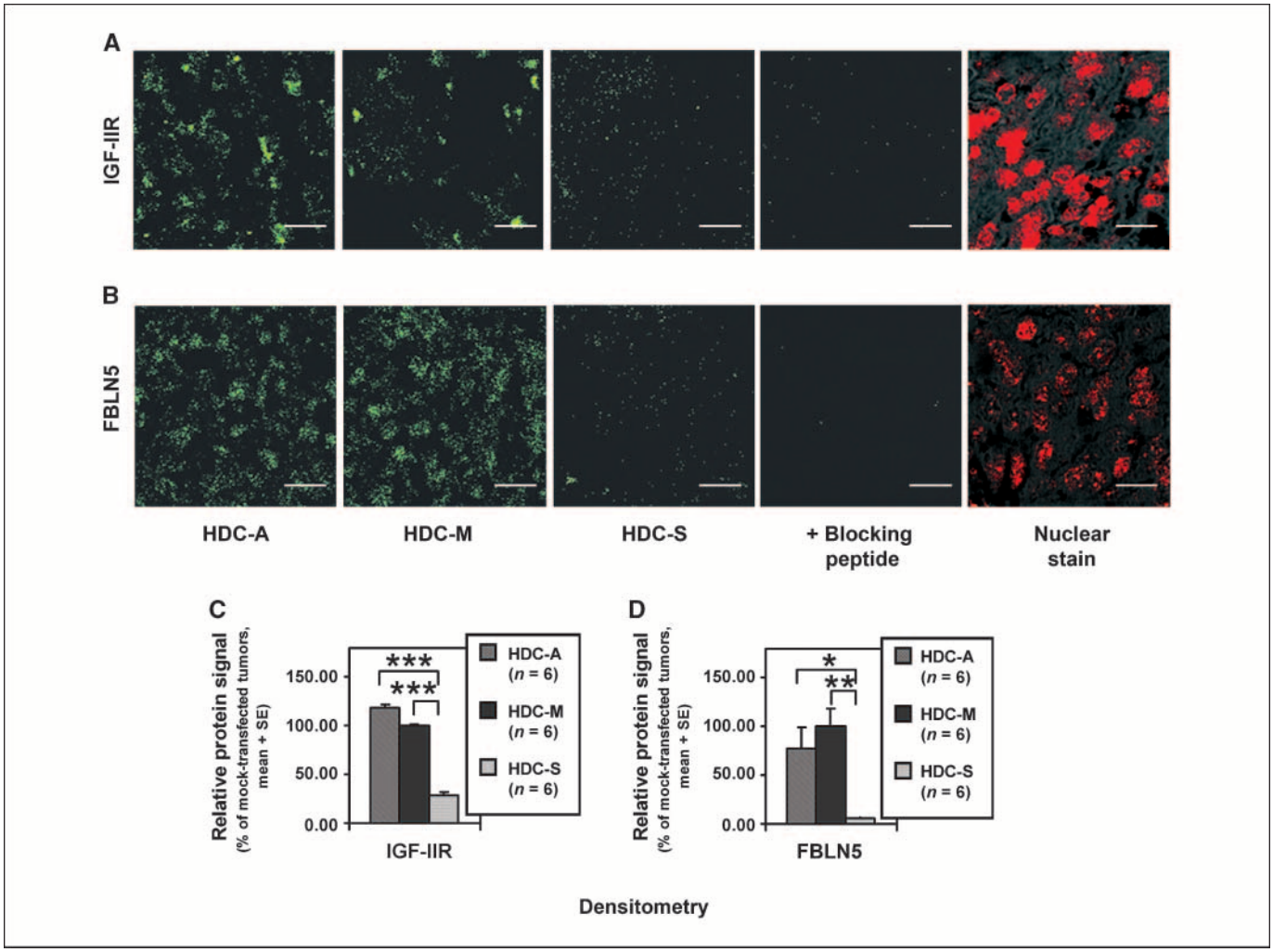

Figure 2. Analysis of IGF-IIR and FBLN5 protein expression in transgenic mouse melanomas with modified histamine secretion. Representative tissue sections displaying typical results of IGF-IIR– (*A, green*) and FBLN5-specific immunohistochemistries (*B, green*) are shown in three transgenic B16-F10 experimental tumors (×400 magnification; *bar,* 10 μm). Result evaluation was done by densitometry (*C* and *D*). *, $P < 0.05$; **, $P < 0.01$; ***, $P < 0.001$, between individual groups as calculated by a Holm-Sidak test.

and B16-F10 HDC-S tumors, secreting decreased, unmodified, and elevated levels of histamine, respectively, were compared using 44K whole genome expression microarrays. A cluster of 45 features was identified (Fig. 1*A*), consisting of genes differently expressed between any of the three different tumor groups and thus significantly affected by the manipulation of melanoma histamine secretion. Genes significantly affected by transfection were found to be evenly dispersed along the mouse genome, suggesting that these changes are not due to a single chromosomal mutation or other artifacts associated to transfection, such as serial trans-activation of structurally coupled genes by the inserted mammalian expression vector (Supplementary data 1). This cluster was then further filtered to identify histamine-dependent signatures and thus markers following the gradually changing histamine levels in the three experimental melanoma groups. An expression signature of 12 features, gradually up-regulated by histamine, and a similar marker set, consisting of 15 array features, all down-modulated by histamine, were identified (Fig. 1*A*).

Validation of microarray results by real-time PCR: focus on histamine-affected genes with known oncogenic potential. Judged by literature searches, histamine-dependent annotated genes, known to be implicated in tumorigenesis or cancer progression, were selected for further evaluation by real-time PCR. This way, we first identified a gene called *RIS2*, which is a licensing factor allowing for DNA replication and thus controlling S-phase entry in dividing cells (17). RIS2 was up-regulated by histamine (Fig. 1*A* and *B*). Second, a similar histamine-dependent up-regulation was measured in the case of ASNS (Fig. 1*A* and *B*). This was similarly interesting because some neoplasms display elevated asparagine demand, and availability of asparagine is a strong growth-limiting factor in these cancers (18).

From markers down-modulated by histamine in microarray experiments, we first identified FBLN5, a small extracellular matrix protein (Fig. 1*A* and *B*). Evidence is available indicating that FBLN5 interferes with angiogenesis, and hence it is often referred to as a bona fide tumor suppressor (19). Gene expression patterns highly similar to FBLN5 were found in the case of IGF-IIR, too (Fig. 1*A* and *B*), which is a tumor-suppressor decoy receptor (20) for IGF-II. IGF-IIR interferes with IGF-II–mediated signaling via its other receptor, IGF-IR, which has paramount importance in many growth-related processes such as embryonic growth or the development of different neoplasms, such as melanoma, as it

mediates strong proliferatory signals for many cell types (21). Finally, we identified CAR13, an enzyme controlling cellular respiration and extracellular matrix stability by modifying local CO_2 concentration and, indirectly, pH. CAR13 was reported to be down-regulated in colon carcinoma (22) and histamine seemed to suppress its expression (Fig. 1*A* and *B*).

To validate microarray results, expression patterns of these genes were evaluated by real-time PCR, too. We found that real-time PCR accurately reproduced microarray results in four of five markers (Fig. 1*C*). One-way ANOVA analysis confirmed reproducible histamine-mediated up-modulation or down-modulation in the case of ASNS ($P = 0.002$), RIS2 ($P = 0.015$), IGF-IIR ($P < 0.001$), and FBLN5 ($P = 0.023$). However, no significant difference was found in the levels of CAR13 ($P = 0.090$), and therefore this gene was omitted from further investigations (see Fig. 1*C* for between-group comparisons by Holm-Sidak test).

Histologic analysis confirms histamine-dependent regulation of IGF-IIR and FBLN5. Protein-level expression and tissue distribution of genes previously validated by real-time PCR were analyzed by immunohistochemistry. As for two markers (IGF-IIR and RIS2), there were no commercial mouse-specific antibodies available; antibodies specific for their human homologues were applied instead. In such cases, cross-reactivity with the respective mouse antigen was checked by Western blotting in pilot studies. An antihuman IGF-IIR antibody showed cross-reactivity with the respective mouse protein, but the antihuman RIS2 antibodies tested by us did not (Supplementary data 2). Therefore, we were not able to follow this marker at the protein level.

After performing immunohistochemistry for IGF-IIR, FBLN5, and ASNS in experimental B16-F10 tumors, we found that ASNS protein expression in these melanomas was not strong enough to be detected reproducibly (not shown). On the contrary, both IGF-IIR and FBLN5 were found to be easily detectable, evenly distributed in the tumor cells, and located mainly intracellularly (Fig. 2*A* and *B*). They showed expression patterns highly similar to their RNA-level expression profile (Fig. 2*C* and *D*), whereas IGF-IIR and FBLN5 proteins were significantly diminished in B16-F10 HDC-S melanomas engineered to secrete elevated levels of histamine ($P < 0.001$ and $P = 0.002$ for IGF-IIR and FBLN5, respectively, both by one-way ANOVA; see Fig. 2*C* and *D* for between-group comparisons by Holm-Sidak test).

Western blotting and histamine receptor functionality assays disclose that histamine affects B16-F10 melanomas via histamine H1R and H2R, but not via H3R or H4R. Our next aim was the identification of the histamine receptor(s) involved in the above alterations in IGF-IIR and FBLN5 levels and the tumor-growth supporting effect of histamine. To this end, we first assessed the expression of all four histamine receptors known to date (H1R, H2R, H3R, and H4R) in B16-F10 tumors. In accordance with our previous observations, suggesting that H1Rs and H2Rs might be the two histamine receptors playing a pivotal role in melanoma growth (16), Western blots disclosed that B16-F10 experimental melanomas display H1R and H2R proteins, but not H3R and H4R, at detectable levels (Fig. 3*A*).

Next, we checked the functional integrity of H1R or H2R on these cells, as well. Treatment of B16-F10 cells with the H1R agonist 2-pyridylethylamine dihydrochloride resulted in elevated intracellular levels of inositol-monophosphate, a stable metabolite of inositol 1,4,5-trisphosphate (23), suggesting that B16-F10 melanomas exhibit fully functional H1Rs (refs. 24, 25; Fig. 3*B*). Similarly, treatment of B16-F10 cells with amthamine dihydrobromide, a specific H2R agonist, led to enhanced intracellular cAMP production, confirming that mouse melanoma cells display functionally intact H2Rs, as well (refs. 24, 25; Fig. 3*C*).

Histamine receptor blockade experiments show that histamine H1R, but not H2R, activation supports B16-F10 melanoma growth. Next, we analyzed the relative importance of H1R- and H2R-mediated signals in the histamine-induced enhanced growth of B16-F10 melanomas. In these experiments, the H1R antagonist loratadine and the H2R anti-histamine famotidine (25) were given to mice bearing experimental B16-F10 tumors. Groups of mice grafted with B16-F10 HDC-S melanomas, characterized by elevated levels of histamine secretion and enhanced tumor growth (16), were treated with different doses of loratadine (+LOR) or vehicle only (−LOR), and it was checked whether this treatment would be capable of neutralizing the growth-promoting effect of histamine. Parallel to this, a similar experiment was conducted comparing mice receiving famotidine (+FAM) with their respective control group vehicle (−FAM; Fig. 4). Both antagonists were administered p.o. at three different doses: in one dose equivalent to their maximal clinically applied daily dosage, and in two additional doses representing ~10 and 100 times higher dosage (26, 27). We found that loratadine effectively neutralized ($P = 0.015$, two-way ANOVA and Holm-Sidak post hoc test) the growth-supporting effect of histamine seen in B16-F10 HDC-S tumors at all applied doses (Fig. 4*B*), approximately returning their growth rate to that of mock-transfected B16-F10 HDC-M control group (Fig. 4*A*). On the contrary, famotidine treatment failed to suppress the enhanced growth of B16-F10 HDC-S grafts (Fig. 4*C*).

Histamine H1R and H2R blockade identifies H1R as the predominant regulator of FBLN5 and IGF-IIR gene expression in B16-F10 melanomas. We next compared mRNA and protein

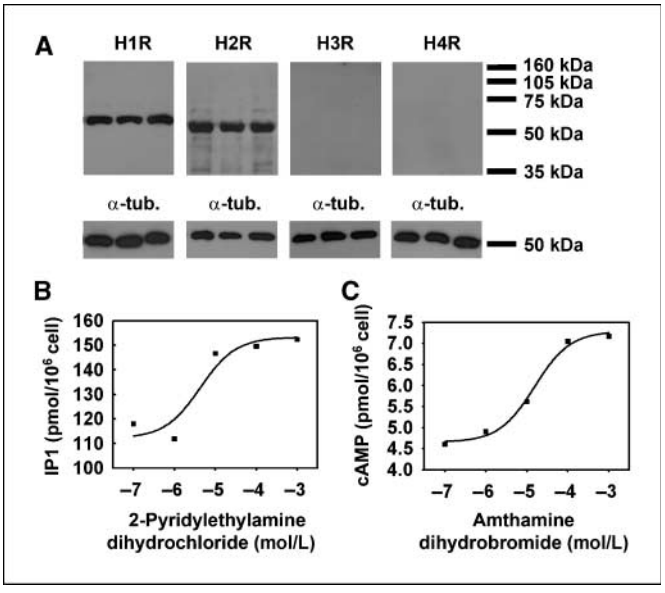

Figure 3. Comprehensive analysis of the expression and functional integrity of all four known histamine receptors in B16-F10 melanomas. *A,* full-length Western blots done on B16-F10 HDC-M tumors aiming the detection of histamine H1R, H2R, H3R, and H4R proteins along with α-tubulin loading controls. *B* and *C,* results of ELISA experiments measuring changes in the intracellular inositol-monophosphate (*IP1*) and cAMP levels of B16-F10 HDC-M cells in response to different doses of a specific H1R agonist and H2R agonist, respectively.

expression levels of IGF-IIR and FBLN5 in experimental melanomas in the absence and presence of the above H1R and H2R antihistamines. Real-time PCR analysis confirmed that blockade of H1Rs alleviated histamine-mediated, mRNA-level suppression of both IGF-IIR ($P = 0.018$, one-way ANOVA) and FBLN5 ($P = 0.004$, Kruskal-Wallis one-way ANOVA on ranks), whereas a blockade of H2Rs did not have any significant effect (see Fig. 4*D* for detailed between-group comparisons by Holm-Sidak test).

In accordance with this, subsequent immunohistochemistry confirmed that H1R-specific antihistamine treatment was able to neutralize histamine-mediated suppression of both IGF-IIR and FBLN5 protein expression ($P = 0.025$ and $P < 0.001$, respectively, Holm-Sidak test after one-way ANOVA; Fig. 5*A* and *B*). Highly interestingly, however, we found that at least at the protein level, H2R antagonist treatment affected the IGF-IIR and FBLN5 content of B16-F10 melanomas similarly to a H1R blockade ($P < 0.001$ for both cases, Holm-Sidak test done after one-way ANOVA; Fig. 5*A* and *B*).

On the other hand, due to the presence of an apparently large intracellular IGF-IIR and FBLN5 protein pool in the cells, the strong intracellular protein staining heavily interfered with reliable quantification of the exported pools of the two proteins. This was an important methodical limitation because both IGF-IIR and FBLN5 exert their tumor-suppressive effects on successful protein export only (19, 20). Therefore, we set up an *in vitro* assay that was able to determine the levels of the membrane-bound form of IGF-IIR and the amounts of secreted FBLN5 without being affected by changes in the intracellular protein pools of these two markers. To this end, B16-F10 HDC-S cells were treated with loratadine and famotidine for 1 week *in vitro*, and the amount of surface IGF-IIR was assessed by flow cytometry, whereas levels of secreted FBLN5 were determined by analyzing concentrated cell culture supernatants by Western blotting. Our results show that in line with the RNA-level gene expression data, loratadine-mediated H1R blockade results in highly elevated levels of membrane-bound IGF-IIR and secreted FBLN5(28, 29), as compared with the untreated control (Fig. 5*C* and *D*). On the contrary, H2R antagonist treatment induced only a minimal increase in the availability of the same proteins (Fig. 5*C* and *D*).

Discussion

In this study, a global survey of the molecular mechanisms of histamine-mediated growth support for melanomas was carried out by high-throughput gene expression profiling. Focusing on histamine-affected genes with known oncogenic potential, we provided convincing evidence that histamine suppresses expression of two tumor suppressor genes, *IGF-IIR* and *FBLN5*, both at the mRNA and protein levels.

IGF-IIR is a multifaceted protein, serving as a transmembrane scavenger receptor for IGF-II, which is a potent growth factor for many dividing cell types and neoplasms. IGF-IIR sequesters IGF-II from potential interactions with its activating receptor, IGF-IR, and rapidly targets it for lysosomal degradation (20). IGF-IIR is a known tumor suppressor as it inhibits growth of both embryonic (30, 31) and tumor cells (32), and the *IGF-IIR* gene displays frequent loss of heterozygosity in several unrelated neoplasms (20). FBLN5 belongs to the family of fibulins, small secreted

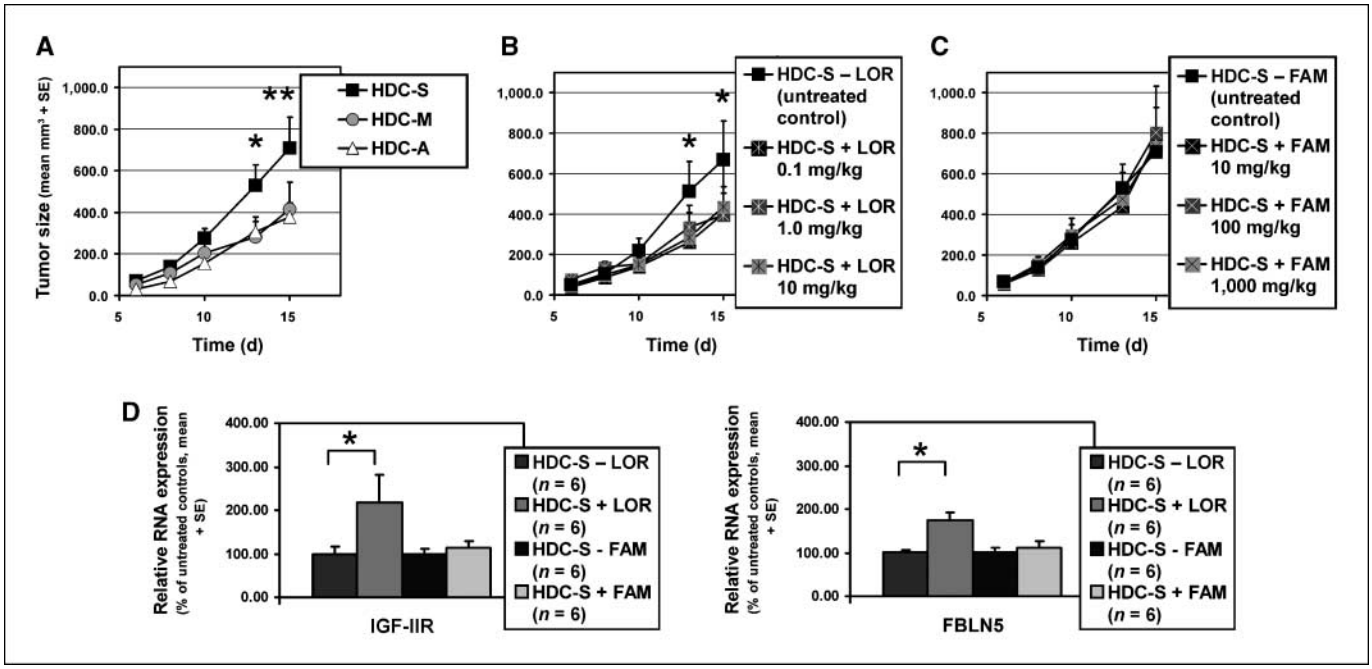

Figure 4. Identification of the histamine receptor responsive for histamine-mediated tumor growth support and suppression of IGF-IIR and FBLN5 mRNA expression in mouse melanomas. *A,* growth rate of experimental melanomas in C57BL/6 mice grafted with stably transfected B16-F10 melanoma cells exhibiting suppressed (HDC-A), unmodified (HDC-M), and enhanced (HDC-S) histamine production. *, $P < 0.05$; **, $P < 0.01$, between the latter two groups (Holm-Sidak post hoc test). *B,* a separate experiment carried out on animals bearing B10-F10 HDC-S tumors, receiving vehicle only (−LOR) or different doses of the H1R antagonist loratadine (+LOR) via drinking water. *C,* a similar experiment analyzing HDC-S tumor growth rate with administration of vehicle (−FAM) or different amounts of the H2R antagonist famotidine (+FAM) to tumor-bearing animals. *, $P < 0.05$, between control and antagonist-treated groups (Holm-Sidak post hoc test). *D,* IGF-IIR and FBLN5 mRNA levels in experimental melanomas of mice treated with the above H1R- and H2R-specific antagonists. *, $P < 0.05$, between control and antagonist-treated groups (Holm-Sidak post hoc test).

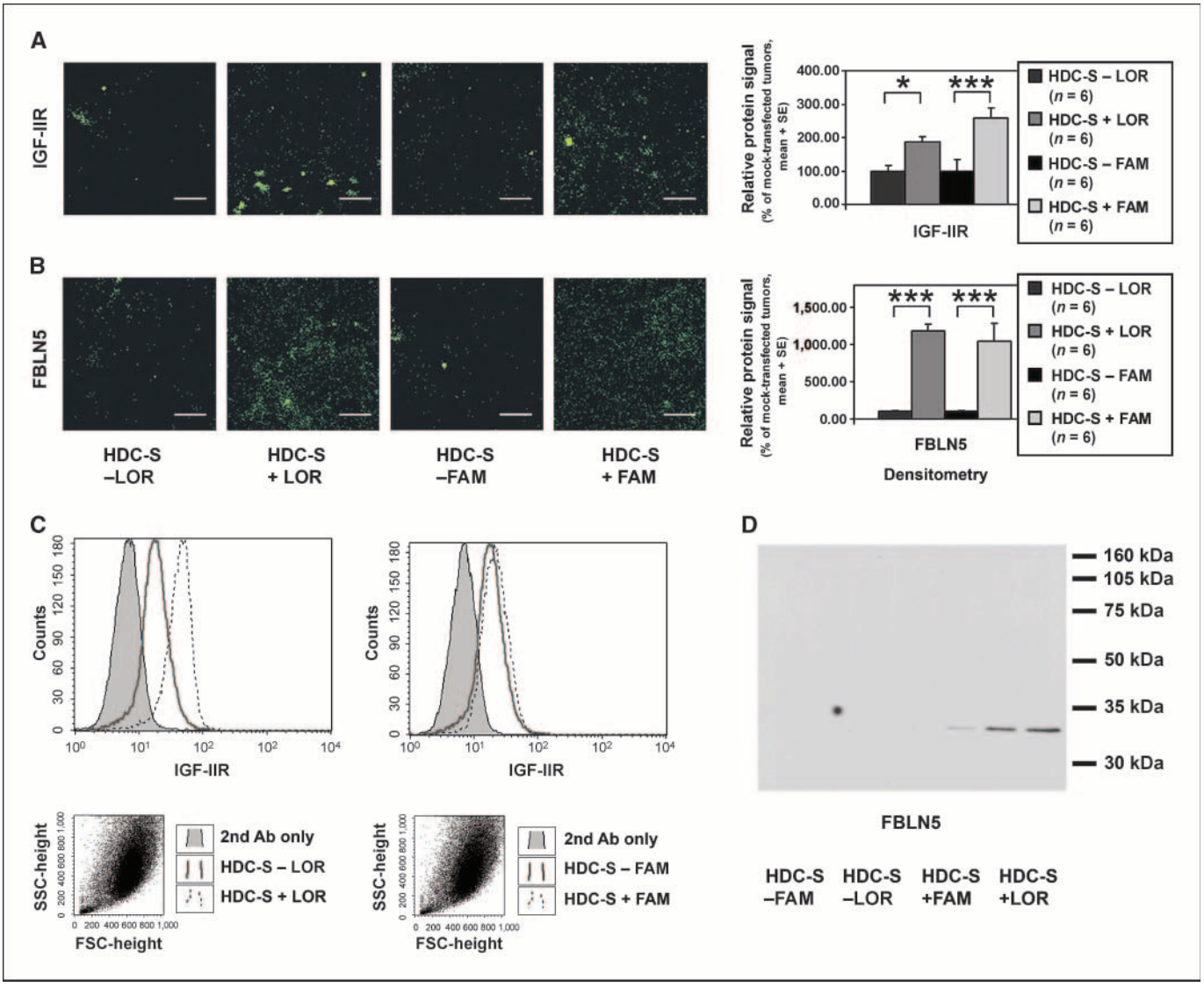

Figure 5. Analysis of the effects of H1R and H2R blockade on total levels and subcellular distribution of IGF-IIR and FBLN5 proteins in melanoma cells. Total IGF-IIR and FBLN5 protein levels were analyzed by immunohistochemistry in mice bearing transgenic B16-F10 HDC-S tumors overproducing histamine. In two separate experiments, tumor-bearing animals received vehicle (−LOR) or the H1R antagonist loratadine (+LOR) and vehicle (+FAM) or the H2R antagonist famotidine (+FAM) via drinking water. Representative tissue sections (×400 magnification; *bar,* 10 μm) displaying typical results of IGF-IIR– (*A, green signal*) and FBLN5-specific immunohistochemistry (*B, green signal*) and statistical evaluation of densitometric image analysis (*A* and *B, right*). *, $P < 0.05$; ***, $P < 0.001$, between control and antagonist-treated groups, as calculated by a Holm-Sidak test. *C* and *D,* presence or absence of IGF-IIR and FBLN5 proteins successfully exported from the same cells treated with famotidine or loratadine *in vitro. C,* representative results of three experiments assessing levels of IGF-IIR displayed on the surface of untreated and antagonist-treated cells *in vitro*, as measured by flow cytometry. *D,* summarized results of two experiments measuring levels of secreted FBLN5 in concentrated supernatants of untreated and antagonist-treated cells by Western blotting.

glycoproteins characterized by a typical rod-shaped morphology. It controls both cell-cell and cell-matrix interactions recognizing the integrins $\alpha_v\beta_3$, $\alpha_v\beta_5$, and $\alpha_9\beta_1$(33) or matrix components such as tropoelastin (34). FBLN5 plays a critical role in normal elastogenesis, vasculogenesis, and tissue repair, and it was shown that FBLN5 heavily interferes with capillary vessel sprouting by suppressing vascular endothelial growth factor signaling, DNA replication, and motility in endothelial cells (35). In addition, FBLN5 is down-regulated in the majority of tumors investigated, particularly in metastatic cancers; hence, it is characterized as a bona fide tumor suppressor (19).

Interestingly, histamine-mediated suppression of IGF-IIR and FBLN5 happens coordinately in our experiments, and indeed, *in silico* pathway analysis identifies IGF-IIR, FBLN5, and many other histamine-affected melanoma genes as members of a single tumor-suppressive gene regulatory cluster (Fig. 6) directed by transforming growth factor β1 (TGFβ1). TGFβ is released by TGFβ-secreting cells in a matrix-bound, latent proprotein form, which has to be cleaved to become activated. It was shown that IGF-IIR is able to bind the urokinase-type plasminogen activator (uPA) receptor and thereby assists in uPA- and plasmin-mediated TGFβ activation (36). Activated TGFβ, on the other hand, is a master enhancer of FBLN5 expression (37). Taken together, these data suggest that histamine coordinately suppresses IGF-IIR and FBLN5 expression because it interferes with IGF-IIR expression, thereby inhibiting conversion of latent TGFβ1 to its active form,

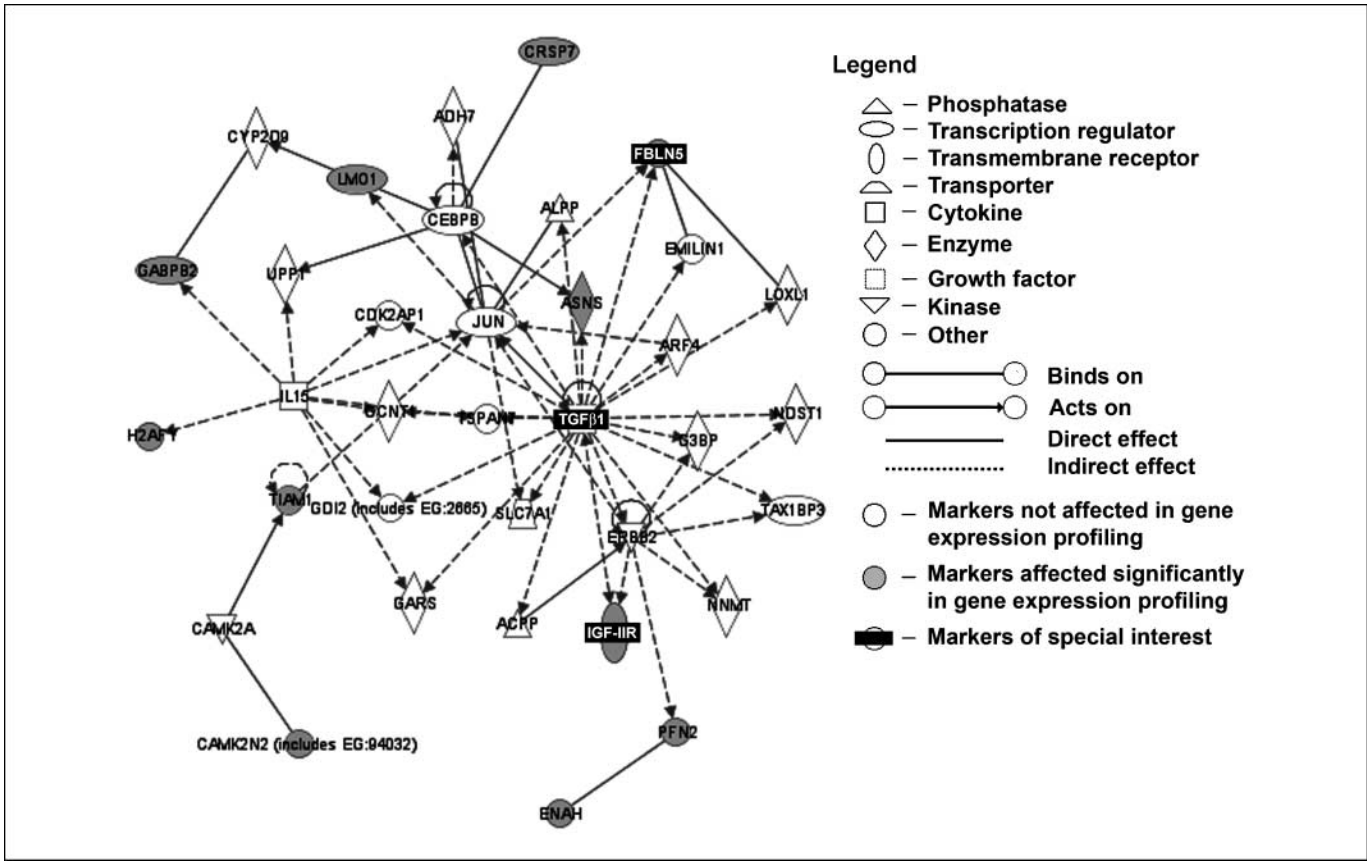

Figure 6. *In silico* pathway analysis of the molecular mechanism of histamine action in mouse melanomas. Microarray gene expression data were analyzed *in silico* with help of the Ingenuity Pathway Analysis (IPA) tool. Gene sets significantly affected by manipulation of B16-F10 histamine secretion in array experiments were analyzed with help of the gene network database of IPA. The gene network getting the highest score, describing a network affecting cancer, cellular growth and proliferation, and gastrointestinal disease, is shown. For detailed information on the displayed genes, see Supplementary data 4.

which in turn results in a diminished expression of FBLN5 mRNA in melanoma cells.

We next showed that H1R, but not H2R, activation is responsive for the enhanced growth rate of mouse melanomas overproducing histamine. Although H2R was reported to be up-regulated by histamine in B16-F10 melanoma (16) and other neoplasms, and it has some clearly tumorigenic effects in melanoma cell lines and other unrelated cancers (38, 39), we showed that it is definitively not sufficient to induce histamine-mediated enhancement of B16-F10 mouse melanoma growth *in vivo*. These unexpected results are clearly not due to an inactivation of the *H2R* gene in B16-F10 melanoma cells because we were able to show that both H1R and H2R are functionally intact and fully active on them.

In line with this, we showed that administration of H1R, but not H2R, antagonists was able to neutralize the suppressive effect of histamine on mRNA level IGF-IIR and FBLN5 expression. This phenomenon was associated with a restoration of intracellular IGF-IIR and FBLN5 pools at the protein level and elevated amounts of plasma membrane–bound IGF-IIR and secreted FBLN5 proteins. These observations suggest that H1R activation exerts a strong suppressive effect on IGF-IIR and FBLN5 gene expression, leading to a subsequent decrease in IGF-IIR and FBLN5 protein levels both in the intracellular compartment and the plasma membrane or the extracellular matrix surrounding melanoma cells. Considering that tumor growth rate strictly followed gene expression patterns of these two proteins, and the proposed tumor-suppressive effect of IGF-IIR and FBLN5, these observations suggest that there is a causative link between the histamine-mediated suppression of FBLN5 and IGF-IIR expression and the enhanced growth of histamine-affected melanoma tumors.

On the other hand, somewhat surprisingly, we also found that although it is completely ineffective in regulating tumor growth, blockade of H2R has similar consequences to a H1R blockade in one particular regard, namely, it strongly elevates IGF-IIR and FBLN5 protein levels within the affected cells. In striking contrast to a H1R blockade, however, H2R antagonist treatment did not result in any changes in the transcription of the *IGF-IIR* and *FBLN5* genes; further, it did not induce striking changes in the amount of IGF-IIR and FBLN5 proteins successfully exported from the intracellular compartment of melanoma cells. In other words, the data show that H2R activation leads to a strong posttranslationally induced decrease, mainly affecting the intracellular protein pool of these two tumor suppressors. Of note, we showed that this effect can be mimicked by H1R activation, which has a similar effect on the intracellular protein pool but acts somewhat upstream, at the RNA level, and leads to a complete phenotype in terms of both reduced IGF-IIR and FBLN5 export and enhanced tumor growth. To sum up, the

above observations suggest a limited relevance for H2R in melanoma, which is in line with the fact that H2R antagonist treatment alone is insufficient to reduce tumor growth in this melanoma model.

Finally, it should be emphasized that IGF-IIR and FBLN5 are probably not the only targets of histamine in melanoma cells. By focusing this study on genes having a known oncogenic potential, we probably missed many relevant targets of histamine in developing melanomas. Hence, further studies are strongly warranted to analyze the remaining pool of histamine-affected but not yet fully annotated genes in melanoma.

Acknowledgments

Received 7/24/2007; revised 11/20/2007; accepted 1/14/2008.

Grant support: Hungarian Medical Research Council Grant ETT no. 138/2006 (Z. Pos, H. Hegyesi, and A. Falus).

The costs of publication of this article were defrayed in part by the payment of page charges. This article must therefore be hereby marked *advertisement* in accordance with 18 U.S.C. Section 1734 solely to indicate this fact.

References

1. Coussens LM, Werb Z. Inflammation and cancer. Nature 2002;420:860–7.
2. Maeda H, Akaike T. Nitric oxide and oxygen radicals in infection, inflammation, and cancer. Biochemistry (Mosc) 1998;63:854–65.
3. Hudson JD, Shoaibi MA, Maestro R, Carnero A, Hannon GJ, Beach DH. A proinflammatory cytokine inhibits p53 tumor suppressor activity. J Exp Med 1999; 190:1375–82.
4. Diegelmann RF, Evans MC. Wound healing: an overview of acute, fibrotic and delayed healing. Front Biosci 2004;9:283–9.
5. Arnott CH, Scott KA, Moore RJ, et al. Tumour necrosis factor-α mediates tumour promotion via a PKCα- and AP-1-dependent pathway. Oncogene 2002;21:4728–38.
6. Muller A, Homey B, Soto H, et al. Involvement of chemokine receptors in breast cancer metastasis. Nature 2001;410:50–6.
7. Strieter RM, Burdick MD, Mestas J, Gomperts B, Keane MP, Belperio JA. Cancer CXC chemokine networks and tumour angiogenesis. Eur J Cancer 2006;42:768–78.
8. Ben Baruch A. Inflammation-associated immune suppression in cancer: the roles played by cytokines, chemokines and additional mediators. Semin Cancer Biol 2006;16:38–52.
9. Jutel M, Blaser K, Akdis CA. The role of histamine in regulation of immune responses. Chem Immunol Allergy 2006;91:174–87.
10. Bartholeyns J, Bouclier M. Involvement of histamine in growth of mouse and rat tumors: antitumoral properties of monofluoromethylhistidine, an enzyme-activated irreversible inhibitor of histidine decarboxylase. Cancer Res 1984;44:639–45.
11. Cricco GP, Davio CA, Martin G, et al. Histamine as an autocrine growth factor in experimental mammary carcinomas. Agents Actions 1994;43:17–20.
12. Tanimoto A, Matsuki Y, Tomita T, Sasaguri T, Shimajiri S, Sasaguri Y. Histidine decarboxylase expression in pancreatic endocrine cells and related tumors. Pathol Int 2004;54:408–12.
13. Haak-Frendscho M, Darvas Z, Hegyesi H, et al. Histidine decarboxylase expression in human melanoma. J Invest Dermatol 2000;115:345–52.
14. Falus A, Hegyesi H, Lazar-Molnar E, Pos Z, Laszlo V, Darvas Z. Paracrine and autocrine interactions in melanoma: histamine is a relevant player in local regulation. Trends Immunol 2001;22:648–52.
15. Hart PH, Grimbaldeston MA, Finlay-Jones JJ. Sunlight, immunosuppression and skin cancer: role of histamine and mast cells. Clin Exp Pharmacol Physiol 2001;28:1–8.
16. Pos Z, Safrany G, Muller K, Toth S, Falus A, Hegyesi H. Phenotypic profiling of engineered mouse melanomas with manipulated histamine production identifies histamine H2 receptor and rho-C as histamine-regulated melanoma progression markers. Cancer Res 2005;65: 4458–66.
17. Arentson E, Faloon P, Seo J, et al. Oncogenic potential of the DNA replication licensing protein CDT1. Oncogene 2002;21:1150–8.
18. Richards NG, Kilberg MS. Asparagine synthetase chemotherapy. Annu Rev Biochem 2006;75:629–54.
19. Albig AR, Schiemann WP. Fibulin-5 function during tumorigenesis. Future Oncol 2005;1:23–35.
20. DaCosta SA, Schumaker LM, Ellis MJ. Mannose 6-phosphate/insulin-like growth factor 2 receptor, a bona fide tumor suppressor gene or just a promising candidate? J Mammary Gland Biol Neoplasia 2000;5:85–94.
21. Maloney EK, McLaughlin JL, Dagdigian NE, et al. An anti-insulin-like growth factor I receptor antibody that is a potent inhibitor of cancer cell proliferation. Cancer Res 2003;63:5073–83.
22. Kummola L, Hamalainen JM, Kivela J, et al. Expression of a novel carbonic anhydrase, CA XIII, in normal and neoplastic colorectal mucosa. BMC Cancer 2005;5:41.
23. Hughes AR, Putney JW, Jr. Metabolism and functions of inositol phosphates. Biofactors 1988;1:117–21.
24. Hill SJ, Ganellin CR, Timmerman H, et al. International Union of Pharmacology. XIII. Classification of histamine receptors. Pharmacol Rev 1997;49:253–78.
25. Lim HD, van Rijn RM, Ling P, Bakker RA, Thurmond RL, Leurs R. Evaluation of histamine H1-, H2-, and H3-receptor ligands at the human histamine H4 receptor: identification of 4-methylhistamine as the first potent and selective H4 receptor agonist. J Pharmacol Exp Ther 2005;314:1310–21.
26. del Cuvillo A, Mullol J, Bartra J, et al. Comparative pharmacology of the H1 antihistamines. J Investig Allergol Clin Immunol 2006;16 Suppl 1:3–12.
27. Howden CW, Tytgat GN. The tolerability and safety profile of famotidine. Clin Ther 1996;18:36–54.
28. Kuang PP, Goldstein RH, Liu Y, Rishikof DC, Jean JC, Joyce-Brady M. Coordinate expression of fibulin-5/DANCE and elastin during lung injury repair. Am J Physiol Lung Cell Mol Physiol 2003;285: L1147–52.
29. Hirai M, Ohbayashi T, Horiguchi M, et al. Fibulin-5/DANCE has an elastogenic organizer activity that is abrogated by proteolytic cleavage *in vivo*. J Cell Biol 2007;176:1061–71.
30. Lau MM, Stewart CE, Liu Z, Bhatt H, Rotwein P, Stewart CL. Loss of the imprinted IGF2/cation-independent mannose 6-phosphate receptor results in fetal overgrowth and perinatal lethality. Genes Dev 1994; 8:2953–63.
31. DeChiara TM, Efstratiadis A, Robertson EJ. A growth-deficiency phenotype in heterozygous mice carrying an insulin-like growth factor II gene disrupted by targeting. Nature 1990;345:78–80.
32. Wise TL, Pravtcheva DD. Delayed onset of Igf2-induced mammary tumors in Igf2r transgenic mice. Cancer Res 2006;66:1327–36.
33. Nakamura T, Lozano PR, Ikeda Y, et al. Fibulin-5/DANCE is essential for elastogenesis *in vivo*. Nature 2002;415:171–5.
34. Yanagisawa H, Davis EC, Starcher BC, et al. Fibulin-5 is an elastin-binding protein essential for elastic fibre development *in vivo*. Nature 2002;415:168–71.
35. Albig AR, Schiemann WP. Fibulin-5 antagonizes vascular endothelial growth factor (VEGF) signaling and angiogenic sprouting by endothelial cells. DNA Cell Biol 2004;23:367–79.
36. Fortunel NO, Hatzfeld A, Hatzfeld JA. Transforming growth factor-β: pleiotropic role in the regulation of hematopoiesis. Blood 2000;96:2022–36.
37. Kuang PP, Joyce-Brady M, Zhang XH, Jean JC, Goldstein RH. Fibulin-5 gene expression in human lung fibroblasts is regulated by TGF-β and phosphatidylinositol 3-kinase activity. Am J Physiol Cell Physiol 2006; 291:C1412–21.
38. Hegyesi H, Horvath B, Pallinger E, Pos Z, Molnar V, Falus A. Histamine elevates the expression of Ets-1, a protooncogen in human melanoma cell lines through H2 receptor. FEBS Lett 2005;579:2475–9.
39. Takahashi K, Tanaka S, Ichikawa A. Effect of cimetidine on intratumoral cytokine expression in an experimental tumor. Biochem Biophys Res Commun 2001;281:1113–9.